

Finite electron crystallites in strong magnetic fields: Precursors of a supersolid?

Yuesong Li, Constantine Yannouleas, and Uzi Landman
School of Physics, Georgia Institute of Technology, Atlanta, Georgia 30332-0430
 (Dated: 27 February 2005)

We show that a supersolid phase, exhibiting simultaneously solid and superfluid behavior, properly describes the finite electron crystallites that form in two-dimensional quantum dots under high magnetic fields. These crystallites rotate already in their ground state and exhibit a nonclassical rotational inertia. They are precursors to a supersolid crystal in the lowest Landau level. We use exact numerical diagonalization, calculations employing analytic many-body wave functions, and a newly derived analytic expression for the total energies that permits calculations for arbitrary number of electrons.

PACS numbers:

The existence of an exotic supersolid crystalline phase with combined solid and superfluid characteristics has been long conjectured [1, 2, 3]. This conjecture was made in relation to solid ^4He . The recent experimental discovery [4] that solid ^4He exhibits a nonclassical (nonrigid) rotational inertia (NCRI [3]) has revived an intense interest [5, 6, 7, 8, 9] in the existence and properties of the supersolid phase.

The supersolid phase is not restricted to bosonic crystals [9, 10]. In this paper, we demonstrate the existence of such a phase in two-dimensional (2D) semiconductor N -electron quantum dots (QDs) under strong perpendicular magnetic fields (B). Central to the concept of a supersolid is the appearance of a NCRI when the crystal is made to rotate [3, 5].

Under a high magnetic field, the electrons confined in a QD localize at the vertices of concentric polygonal rings and form a rotating electron crystallite (REC) [11, 12]. The ground-state many-electron wave function has a nonzero good total angular momentum quantum number. We show that the corresponding rotational inertia strongly deviates from the rigid classical value, a fact that endows the REC with supersolid characteristics. The REC at high B can be viewed as the precursor of a supersolid crystal that develops in the lowest Landau level (LLL) in the thermodynamic limit. These conclusions were enabled by the development of an analytic expression for the energy of the REC that permits calculations for an arbitrary number of electrons, given the classical polygonal-ring structure in the QD [13].

For strong B we can approximate [14] the single-electron wave function by (parameter free) displaced Gaussian functions; namely, for an electron localized at \mathbf{R}_j (Z_j), we use [14] the expression

$$u(z, Z_j) = \frac{1}{\sqrt{\pi}\lambda} \exp\left(-\frac{|z - Z_j|^2}{2\lambda^2} - i\varphi(z, Z_j; B)\right), \quad (1)$$

with $\lambda = \sqrt{\hbar/m^* \Omega}$; $\Omega = \sqrt{\omega_0^2 + \omega_c^2}/4$, where $\omega_c = eB/(m^*c)$ is the cyclotron frequency and ω_0 specifies the external parabolic confinement defining the QD. The position variables are given by the complex num-

ber $z = x + iy$ and $Z_j = X_j + iY_j$. The phase guarantees gauge invariance in the presence of a perpendicular magnetic field and is given in the symmetric gauge by $\varphi(z, Z_j; B) = (xY_j - yX_j)/2l_B^2$, with $l_B = \sqrt{\hbar c/eB}$ being the magnetic length.

For an extended 2D system, the Z_j 's form a triangular lattice [15]. For finite N , however, the Z_j 's coincide [11, 14, 16] with the equilibrium positions [forming r concentric regular polygons denoted as (n_1, n_2, \dots, n_r)] of $N = \sum_{q=1}^r n_q$ classical point charges inside an external parabolic confinement [13]. The wave function of the *static* electron crystallite (SEC) is a *single* Slater determinant $|\Psi^{\text{SEC}}[z]\rangle$ made out of the single-electron wave functions $u(z_i, Z_i)$, $i = 1, \dots, N$.

$|\Psi^{\text{SEC}}[z]\rangle$ represents a broken-symmetry state, since it is not an eigenstate of the total angular momentum operator with eigenvalue L . For a *rotating* electron crystallite, L must be a good quantum number. To describe the rotation of the electron crystallite, we project the Slater determinant onto a state with good L [11, 14, 16, 17], thus restoring the circular symmetry and obtaining

$$|\Phi_L^{\text{REC}}\rangle = \int_0^{2\pi} \dots \int_0^{2\pi} d\gamma_1 \dots d\gamma_r \times |\Psi^{\text{SEC}}(\gamma_1, \dots, \gamma_r)\rangle \exp\left(i \sum_{q=1}^r \gamma_q L_q\right). \quad (2)$$

Here $L = \sum_{q=1}^r L_q$ and $|\Psi^{\text{SEC}}[\gamma]\rangle$ is the original Slater determinant with *all the single-electron wave functions of the q th ring* rotated (collectively, i.e., coherently) by the *same* azimuthal angle γ_q . Note that Eq. (2) can be written as a product of projection operators acting on the original Slater determinant [i.e., on $|\Psi^{\text{SEC}}(\gamma_1 = 0, \dots, \gamma_r = 0)\rangle$]. Setting $\lambda = l_B \sqrt{2}$ restricts the single-electron wave function in Eq. (1) to be entirely in the lowest Landau level [11]. The continuous-configuration-interaction form of the projected wave functions [i.e., the linear superposition of determinants in Eq. (2)] implies a highly entangled state. We require here that B is sufficiently strong so that all the electrons are spin-polarized and that the ground-state angular momentum

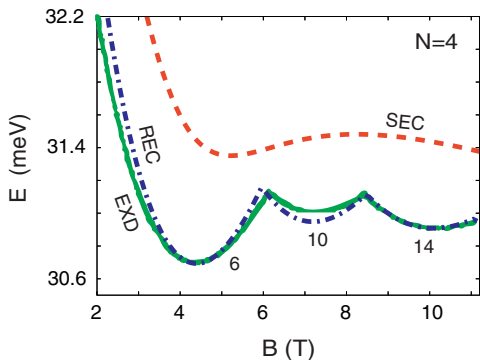


FIG. 1: Ground-state energies calculated with the REC wave function compared to EXD calculations. Energies for $N = 4$ fully polarized electrons (referenced to $4\hbar\Omega$) as a function of the magnetic field B . Dashed line (online red): Broken-symmetry SEC. Solid line (online green): EXD (from Ref. [18]). Dashed-dotted line (online blue): Symmetry-restored REC. Numbers under the curve denote the value of magic angular momenta L_m of the ground state. Corresponding fractional filling factors are specified by $\nu = N(N-1)/(2L_m)$. Parameters used: confinement $\hbar\omega_0 = 3.60$ meV, dielectric constant $\kappa = 13.1$, effective mass $m^* = 0.067m_e$.

$L \geq L_0 \equiv N(N-1)/2$ [the minimum value L_0 specifies the so-called maximum density droplet].

The energy of the REC state [Eq. (2)] is given by [14, 16]

$$E_L^{\text{REC}} = \int_0^{2\pi} h([\gamma]) e^{i[\gamma] \cdot [L]} d[\gamma] / \int_0^{2\pi} n([\gamma]) e^{i[\gamma] \cdot [L]} d[\gamma], \quad (3)$$

with $h([\gamma]) = \langle \Psi^{\text{SEC}}([0]) | H | \Psi^{\text{SEC}}([\gamma]) \rangle$, $n([\gamma]) = \langle \Psi^{\text{SEC}}([0]) | \Psi^{\text{SEC}}([\gamma]) \rangle$, and $[\gamma] \cdot [L] = \sum_{q=1}^r \gamma_q L_q$. The SEC energies are simply given by $E_{\text{SEC}} = h([0])/n([0])$. The many-body Hamiltonian is

$$H = \sum_{i=1}^N \frac{1}{2m^*} \left(\mathbf{p}_i - \frac{e}{c} \mathbf{A}_i \right)^2 + \sum_{i=1}^N \frac{m^*}{2} \omega_0^2 \mathbf{r}_i^2 + \sum_{i=1}^N \sum_{j>i}^N \frac{e^2}{\kappa r_{ij}}, \quad (4)$$

which describes N electrons (interacting via a Coulomb repulsion) confined by a parabolic potential of frequency ω_0 and subjected to a perpendicular magnetic field B , whose vector potential is given in the symmetric gauge by $\mathbf{A}(\mathbf{r}) = \frac{1}{2}(-By, Bx, 0)$. m^* is the effective electron mass, κ is the dielectric constant of the semiconductor material, and $r_{ij} = |\mathbf{r}_i - \mathbf{r}_j|$. For sufficiently high magnetic fields, the electrons are fully spin-polarized and the Zeeman term (not shown here) does not need to be considered.

Prior to demonstrating that the REC wave function [Eq. (2)] exhibits supersolid characteristics, we address the numerical accuracy of its energies [E_L^{REC} in Eq. (3)] compared to exact diagonalization (EXD) solutions of the many-body problem defined by the Hamiltonian in Eq. (4). In Fig. 1, the ground-state energies as a function of

B are compared to EXD calculations [18] for a QD with $N = 4$ electrons. The thick dotted line (online red) represents the broken-symmetry SEC approximation, varying smoothly with B and lying above the EXD curve [solid (online green)]. The REC curve [dashed-dotted (online blue)] agrees well with the EXD one in the entire range $2 \text{ T} < B < 11 \text{ T}$. The REC and EXD ground-state energies exhibit oscillations as a function of B . These oscillations reflect the incompressibility of the many-body states associated with magic angular momenta L_m . The L_m 's are specified by the number of electrons on each polygonal ring; in general $L_m = L_0 + \sum_{q=1}^r k_q n_q$, with k_q being nonnegative integers, i.e., $L_m = 6 + 4k_2$ for the (0,4) structure of $N = 4$, see Fig. 1.

As a second accuracy test, we compare in TABLE I REC and EXD results for the interaction energies of the yrast band for $N = 6$ electrons in the lowest Landau level (an yrast state is the lowest energy state for a given L_m). The relative error is smaller than %0.3, and it decreases steadily for larger L values. The total energy of the REC is lower than that of the SEC, Fig. 1. A theorem discussed in Sec. III of Ref. [19], pertaining to the energies of projected wave functions, guarantees that this lowering of energy applies for all values of N and B .

The crystalline polygonal-ring arrangement (n_1, n_2, \dots, n_r) of classical point charges is portrayed directly in the electron density of the broken-symmetry SEC, since the latter consists of humps centered at the localization sites Z_j 's (*one hump* for each electron). In contrast, the REC has good angular momentum and thus its electron density is circularly uniform. To probe the crystalline character of the REC, we use the

TABLE I: Comparison of yrast-band energies obtained from REC and EXD calculations for $N = 6$ electrons in the lowest Landau level, that is in the limit $B \rightarrow \infty$. In this limit the external confinement can be neglected and only the interaction energy contributes to the yrast-band energies. Energies in units of $e^2/(\kappa l_B)$. For the REC results, the (1,5) polygonal-ring arrangement was considered. For $L < 140$, see TABLE IV in Ref. [11(b)] and Table III in Ref. [23].

L	REC	EXD	Error (%)
140	1.6059	1.6006	0.33
145	1.5773	1.5724	0.31
150	1.5502	1.5455	0.30
155	1.5244	1.5200	0.29
160	1.4999	1.4957	0.28
165	1.4765	1.4726	0.27
170	1.4542	1.4505	0.26
175	1.4329	1.4293	0.25
180	1.4125	1.4091	0.24
185	1.3929	1.3897	0.23
190	1.3741	1.3710	0.23
195	1.3561	1.3531	0.22
200	1.3388	1.3359	0.21

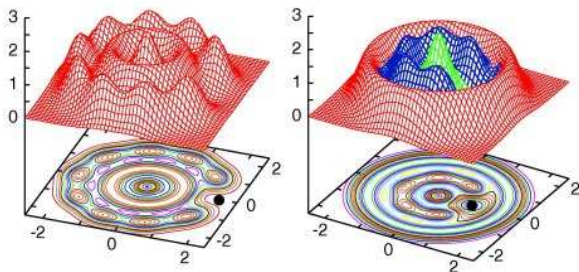


FIG. 2: CPDs for the ground state of $N = 17$ electrons at $B = 10$ T ($L = 228$). The observation point (solid dot) is placed (i) on the outer ring at $r_0 = 1.858R_0$, left frame, and (ii) on the inner ring at $r_0 = 0.969R_0$, right frame. The rest of the parameters are the same as in Fig. 1. Lengths in units of $R_0 = (2e^2/(\kappa m^* \omega_0^2))^{1/3}$. CPDs (vertical axes) in arbitrary units.

conditional probability distribution (CPD) defined as

$$P(\mathbf{r}, \mathbf{r}_0) = \langle \Phi | \sum_{i \neq j} \delta(\mathbf{r}_i - \mathbf{r}) \delta(\mathbf{r}_j - \mathbf{r}_0) | \Phi \rangle / \langle \Phi | \Phi \rangle, \quad (5)$$

where $\Phi(\mathbf{r}_1, \mathbf{r}_2, \dots, \mathbf{r}_N)$ denotes the many-body wave function under consideration. $P(\mathbf{r}, \mathbf{r}_0)$ is proportional to the conditional probability of finding an electron at \mathbf{r} , given that another electron is assumed at \mathbf{r}_0 . This procedure subtracts the collective rotation in the laboratory frame of reference, and, as a result, the CPDs reveal the structure of the many body state in the intrinsic (rotating) reference frame.

In Fig. 2, we display the CPD for the REC wave function of $N = 17$ electrons. This case has a nontrivial three-ring structure (1,6,10) [13], which is sufficiently complex to allow generalizations for larger numbers of particles. The remarkable combined character (partly crystalline and partly fluid leading to a NCRI) of the REC is illustrated in the CPDs of Fig. 2. Indeed, as the two CPDs (reflecting the choice of taking the observation point \mathbf{r}_0 in Eq. (5)) on the outer, left frame, or the inner ring, right frame) reveal, the polygonal electron rings rotate *independently* of each other. Thus, e.g., to an observer located on the inner ring, the outer ring will appear as uniform, and vice versa. The wave functions obtained from exact diagonalization exhibit also the property of independently rotating rings (see e.g., the $N = 9$ case in Ref. [16]), which is a testimony to the ability of the REC wave function to capture the essential physics of a finite number of electrons in high B .

In addition to the conditional probabilities, the solid/fluid character of the REC is revealed in its excited rotational spectrum for a given B . From our microscopic calculations based on the wave function in Eq. (2), we have derived (see below) an approximate (denoted as “app”), but *analytic* and *parameter-free*, expression [see Eq. (8)] which reflects directly the nonrigid (nonclassical) character of the REC for arbitrary size. This expression

allows calculation of the energies of RECs for arbitrary N , given the corresponding equilibrium configuration of confined classical point charges.

We focus on the description of the yrast band at a given B . Motivated by the aforementioned nonrigid character of the rotating electron crystallite, we consider the following kinetic-energy term appropriate for a $(n_1, \dots, n_q, \dots, n_r)$ configuration (with $\sum_{q=1}^r n_q = N$):

$$E_{\text{app}}^{\text{kin}}(N) = \sum_{q=1}^r \hbar^2 L_q^2 / (2\mathcal{J}_q(a_q)) - \hbar\omega_c L / 2, \quad (6)$$

where L_q is the partial angular momentum associated with the q th ring and the total $L = \sum_{q=1}^r L_q$. $\mathcal{J}_q(a_q) \equiv n_q m^* a_q^2$ is the rotational inertia of each *individual* ring, i.e., the moment of inertia of n_q classical point charges on the q th polygonal ring of radius a_q . To obtain the total energy, E_L^{REC} , we include also the term $E_{\text{app}}^{\text{hc}}(N) = \sum_{q=1}^r \mathcal{J}_q(a_q) \Omega^2 / 2$ due to the effective harmonic confinement Ω [see discussion of Eq. (1)], as well as the interaction energy $E_{\text{app}}^{\text{C}}$,

$$E_{\text{app}}^{\text{C}}(N) = \sum_{q=1}^r \frac{n_q S_q}{4} \frac{e^2}{\kappa a_q} + \sum_{q=1}^{r-1} \sum_{s>q}^r V_C(a_q, a_s). \quad (7)$$

The first term is the Coulomb repulsion of n_q point-like electrons on a given ring, with $S_q = \sum_{j=2}^{n_q} (\sin[(j-1)\pi/n_q])^{-1}$, and the second term is the Coulomb repulsion between (uniform) rings with $V_C(a_q, a_s) = n_q n_s {}_2F_1[3/4, 1/4; 1; 4a_q^2 a_s^2 (a_q^2 + a_s^2)^{-2}] e^2 (a_q^2 + a_s^2)^{-1/2} / \kappa$, where ${}_2F_1$ is the hypergeometric function.

For large L (and/or B), the radii of the rings of the rotating crystallite can be found by neglecting the interaction term in the total approximate energy, thus minimizing only $E_{\text{app}}^{\text{kin}}(N) + E_{\text{app}}^{\text{hc}}(N)$. One finds $a_q = \lambda \sqrt{L_q/n_q}$; the ring radii depend on L_q , reflecting the *lack of radial rigidity*. Substitution into the above expressions for $E_{\text{app}}^{\text{kin}}$, $E_{\text{app}}^{\text{hc}}$, and $E_{\text{app}}^{\text{C}}$ yields for the total approximate energy the final expression:

$$E_{\text{app},L}^{\text{REC}}(N) = \hbar(\Omega - \omega_c/2)L + \sum_{q=1}^r \frac{C_{V,q}}{L_q^{1/2}} + \sum_{q=1}^{r-1} \sum_{s>q}^r V_C(\lambda \sqrt{\frac{L_q}{n_q}}, \lambda \sqrt{\frac{L_s}{n_s}}), \quad (8)$$

where the constants $C_{V,q} = 0.25 n_q^{3/2} S_q e^2 / (\kappa \lambda)$. In the case of the simplest $(0, N)$ and $(1, N-1)$ ring configurations, Eq. (8) reduces to the partial expressions reported earlier [14, 20].

In Fig. 3 (left frame), and for a sufficiently high magnetic field (e.g., $B = 100$ T such that the Hilbert space of the system reduces to the lowest Landau level), we compare the approximate analytic energies $E_{\text{app},L}^{\text{REC}}$ with the microscopic energies E_L^{REC} calculated from Eq. (3) using the same parameters as in Fig. 1. The agreement

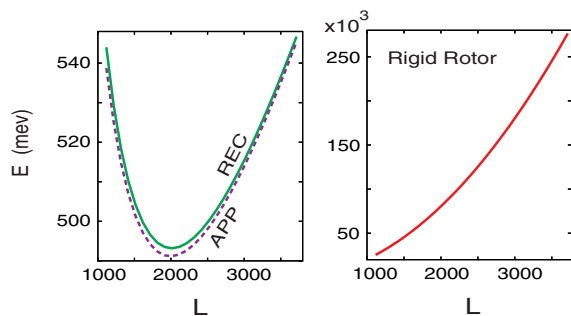


FIG. 3: Left: Approximate analytic expression [Eq. (8), dashed line (online violet)] compared with microscopic REC calculations [Eq. (3), solid line (online green)] for $N = 17$ electrons at high magnetic field. Right: The corresponding classical (rigid rotor) energy E_L^{rig} for $N = 17$ electrons (see text). The microscopic REC energies are referenced relative to the zero-point energy, $17\hbar\Omega$. Energies were calculated for magic angular momenta $L = L_1 + L_2 + L_3$ with $L_1 = 0$, $L_2 = 21 + 6k_2$ and $k_2 = 30$, and $L_3 = 115 + 10k_3$. The parameters are the same as in Fig. 1 and $B = 100$ T. Note the much larger energy scale for the classical case (right frame), leading to a superfluidity index for the REC of $\alpha_s \sim 0.99$ (see text).

is very good (typically less than 0.5%). More important is the strong discrepancy between these results and the total energies E_L^{rig} of the *classical* (rigid rotor) crystallite, plotted in the right frame of Fig. 3; the latter are given by $E_L^{\text{rig}} = \hbar^2 L^2 / (2\mathcal{J}_{\text{rig}}) + 0.5 \sum_{i=1}^N m^* \omega_0^2 |Z_i|^2 + \sum_{i=1}^N \sum_{j>i}^N e^2 / (\kappa |Z_i - Z_j|)$, with the rigid moment of inertia being $\mathcal{J}_{\text{rig}} = \sum_{i=1}^N m^* |Z_i|^2$ [21].

The disagreement between the REC and classical energies is twofold: (i) The L dependence is different, and (ii) The REC energies are three orders of magnitude smaller than the classical ones. That is, the energy cost for the rotation of the REC is drastically smaller than for the classical rotation, thus exhibiting “superfluid” behavior. In analogy with Ref. [3], we define a superfluidity index $\alpha_s = (E_L^{\text{rig}} - E_L^{\text{REC}}) / E_L^{\text{rig}}$. For the case displayed in Fig. 3, we find that this index varies (for $1116 \leq L \leq 3716$) from $\alpha_s = 0.978$ to $\alpha_s = 0.998$, indicating that the REC is highly superfluidic.

Formation of a supersolid is often expected in conjunction with the presence of (i) real defects and (ii) real vacancies [1, 2]. Our supersolid wave function [Eq. 2] belongs to a third possibility, namely to *virtual* defects and vacancies when the number of particles equals the number of lattice sites (the possibility of a supersolid with equal number of particles and lattice sites is mentioned in Ref. [5]). Indeed, the azimuthal shift of the electrons by $(\gamma_1, \gamma_2, \dots, \gamma_r)$ [see Eq. (2)] may be viewed as generating *virtual* defects and vacancies with respect to the original electron positions at $(\gamma_1 = 0, \gamma_2 = 0, \dots, \gamma_r = 0)$.

A recent publication [22] has explored the quantal nature of the 2D electron crystallites in the lowest Lan-

dau level ($B \rightarrow \infty$) using a modification of the second-quantized LLL form of the REC wave functions [11]. In particular, the modification consisted of a multiplication of the *parameter free* REC wave function by variationally adjustable Jastrow-factor vortices. Without consideration of the rotational properties of the modified wave function, the inherently quantal nature of the crystallite was attributed exclusively to the Jastrow factor. However, as shown above, the original REC wave function [Eq. (2)] already exhibits the characteristic NCRI behavior of a supersolid. Consequently, the additional *variational* freedom introduced by the Jastrow prefactor may well lead energetically to a slight numerical improvement, but it does not underlie the physics related to the supersolid behavior. Indeed, the essential step is the projection of the static electron crystallite onto a state with good total angular momentum [see Eqs. (1) and (2)].

In summary, we have shown that rotating electron crystallites, formed in 2D quantum dots under high magnetic fields, exhibit nonclassical rotational inertia which is the signature of a supersolid [3, 5]. We have utilized an analytic many-body wave function [Eq. (2)] which allowed us to carry out computations for a sufficiently large number of electrons ($N = 17$ electrons having a nontrivial three-ring polygonal structure), leading to the derivation and validation of an analytic expression for the total energy of rotating electron crystallites of arbitrary N . These crystallites may be regarded as the precursors of an extended 2D fermionic supersolid in the lowest Landau level.

This research is supported by the US D.O.E. and the NSF.

-
- [1] A.F. Andreev and I.M. Lifshitz, Sov. Phys. JETP **29**, 1107 (1969).
 - [2] G.V. Chester, Phys. Rev. A **2**, 256 (1970).
 - [3] A.J. Leggett, Phys. Rev. Lett. **25**, 1543 (1970).
 - [4] E. Kim and M.H.W. Chan, Nature **427**, 225 (2004); Science **305**, 1941 (2004).
 - [5] T. Leggett, Science **305**, 1921 (2004).
 - [6] M. Tiwari and A. Datta, cond-mat/0406124.
 - [7] N. Prokof'ev and B. Svistunov, cond-mat/0409472.
 - [8] D.M. Ceperley and B. Bernu, Phys. Rev. Lett. **93**, 155303 (2004).
 - [9] H. Falakshahi and X. Waintal, Phys. Rev. Lett. **94**, 046801 (2005).
 - [10] G. Katomeris, F. Selva, and J.-L. Pichard, Eur. Phys. J. B **31**, 401 (2003).
 - [11] C. Yannouleas and U. Landman, (a) Phys. Rev. B **66**, 115315 (2002); (b) Phys. Rev. B **68**, 035326 (2003).
 - [12] The REC is also referred to as rotating electron molecule (REM) or rotating Wigner molecule (RWM).
 - [13] M. Kong, B. Partoens, and F.M. Peeters, Phys. Rev. E **65**, 046602 (2002).
 - [14] C. Yannouleas and U. Landman, Phys. Rev. B **69**, 113306 (2004).

- [15] D.J. Yoshioka and P.A. Lee, Phys. Rev. B **27**, 4986 (1983).
- [16] C. Yannouleas and U. Landman, Phys. Rev. B **70**, 235319 (2004).
- [17] For zero magnetic field, see C. Yannouleas and U. Landman, J. Phys.: Condens. Matter **14**, L591 (2002).
- [18] W.Y. Ruan and H.-F. Cheung, J. Phys.: Condens. Matter **11**, 435 (1999).
- [19] P.-O. Löwdin, Rev. Mod. Phys. **34**, 520 (1962).
- [20] P.A. Maksym, Phys. Rev. B **53**, 10 871 (1996).
- [21] For the classical equilibrium structure of $N = 17$ point charges, the inner radius is $0.9696R_0$, while the outer one is $1.8418R_0$ [13].
- [22] C.-C. Chang, G.S. Jeon, and J.K. Jain, Phys. Rev. Lett. **94**, 016809 (2005).
- [23] C. Yannouleas and U. Landman, Phys. Rev. B **68**, 035325 (2003).